

Supplementary Information

Structure of the VP16 Transactivator Target in ARC/Mediator

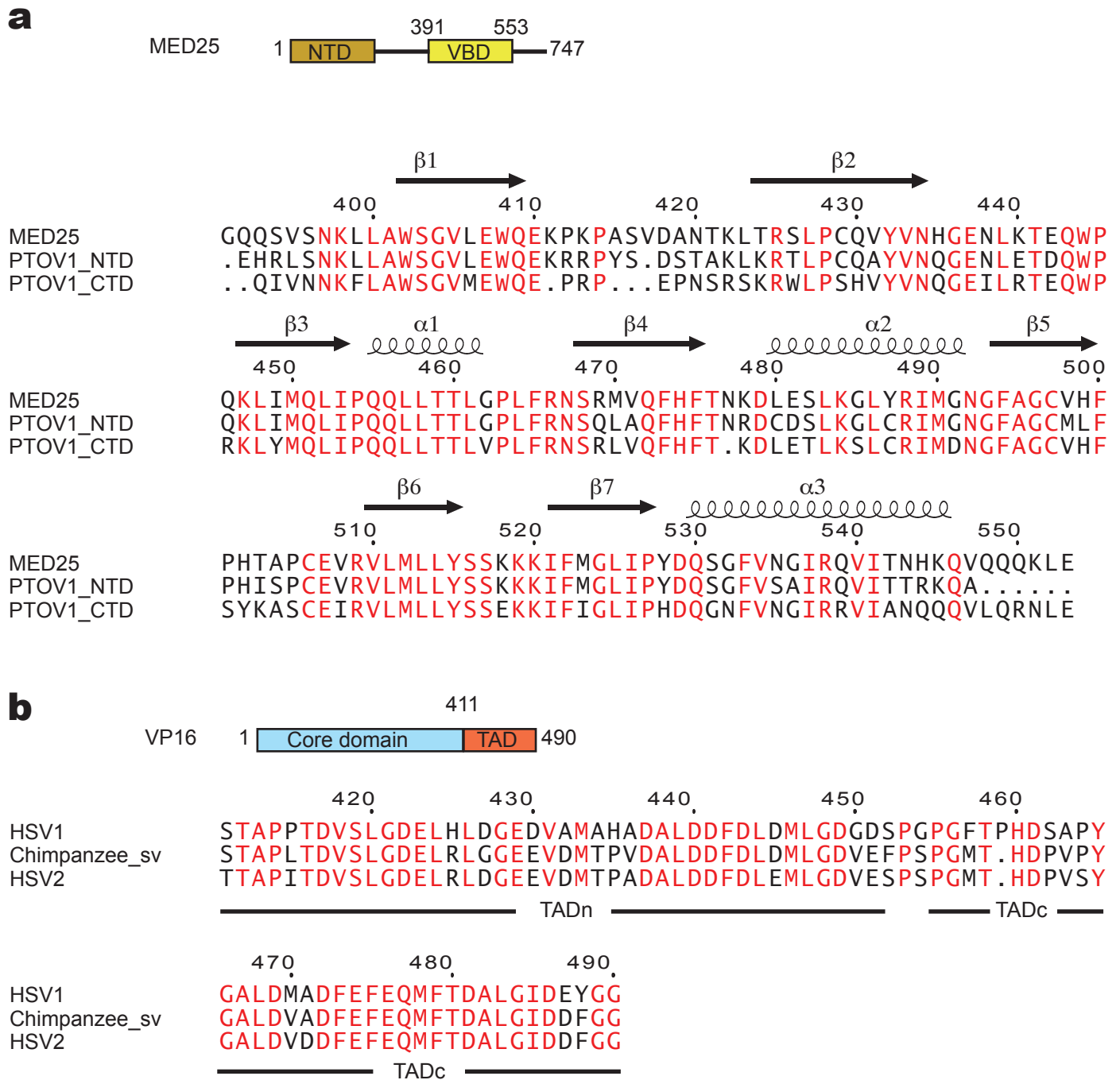
Alexander G. Milbradt¹, Madhura Kulkarni^{2,3*}, Tingfang Yi^{1*}, Koh Takeuchi^{1,4}, Zhen-Yu J. Sun¹,
Rafael E. Luna¹, Philipp Selenko^{1,4}, Anders M. Näär^{2,3} and Gerhard Wagner¹

¹*Department of Biological Chemistry and Molecular Pharmacology, Harvard Medical School, 240 Longwood Avenue, Boston, MA 02115, ²Massachusetts General Hospital Cancer Center, Building 149, 13th Street, Charlestown, MA 02129, ³Department of Cell Biology, Harvard Medical School, 240 Longwood Avenue, Boston, MA 02115.*

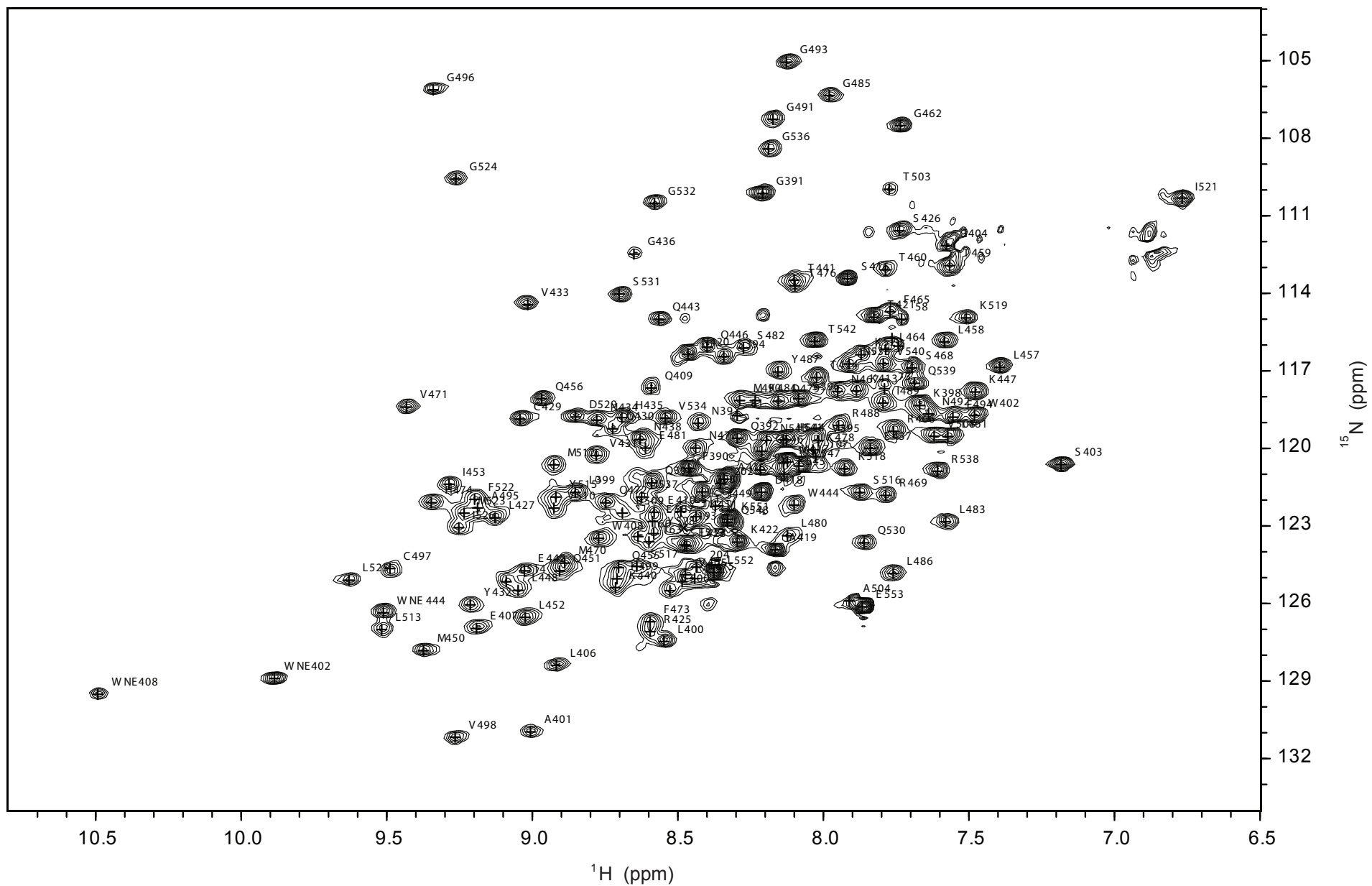
⁴Present addresses: Biomedical Information Research Center, National Institute of Advanced Industrial Science and Technology, Aomi 2-3-26, Koto, Tokyo, 135-0064 Japan
Koh-takeuchi@aist.go.jp, T.K.; Leibniz Institute of Molecular Pharmacology (FMP) Department of NMR-assisted Structural Biology Robert-Roessle-Strasse 10 13125 Berlin, Germany
selenko@fmp-berlin.de, P.S.

* These authors contributed equally to this work.

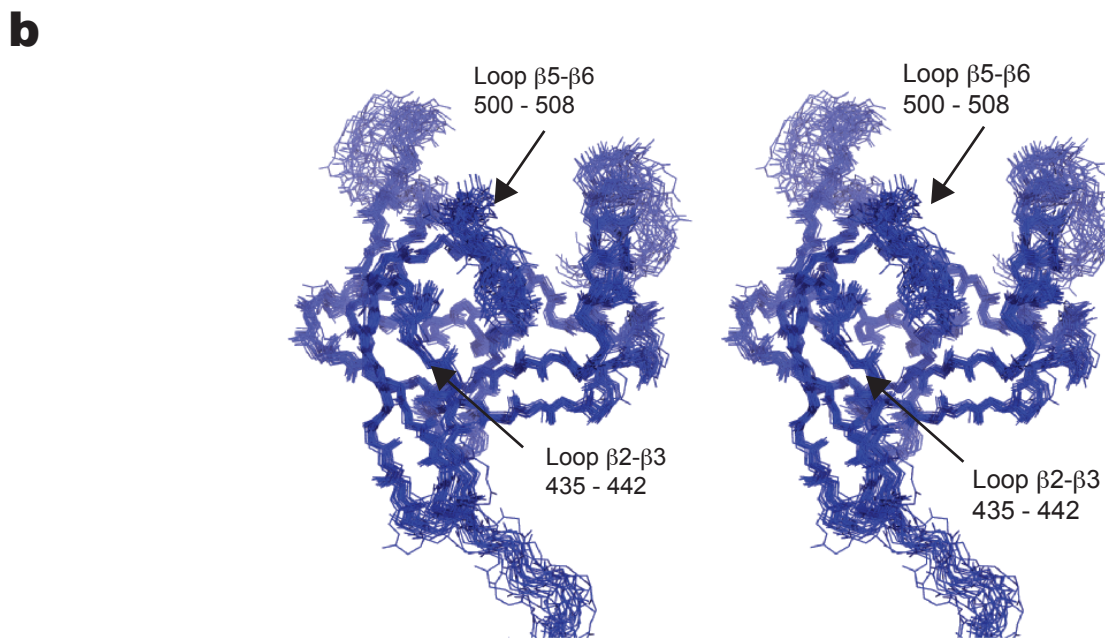
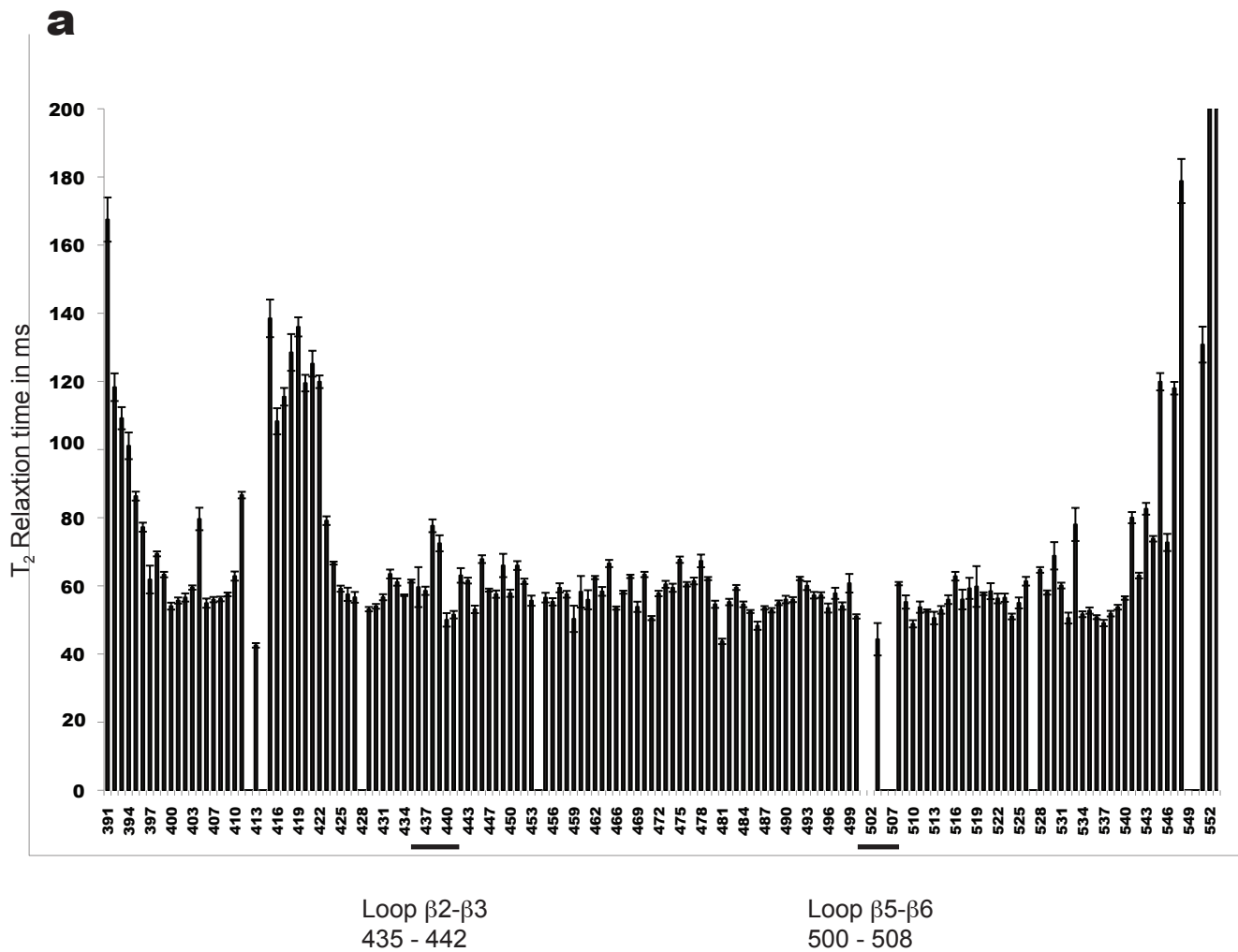
Correspondence should be addressed to A.M.N. (naar@helix.mgh.harvard.edu) or G.W. (gerhard_wagner@hms.harvard.edu).



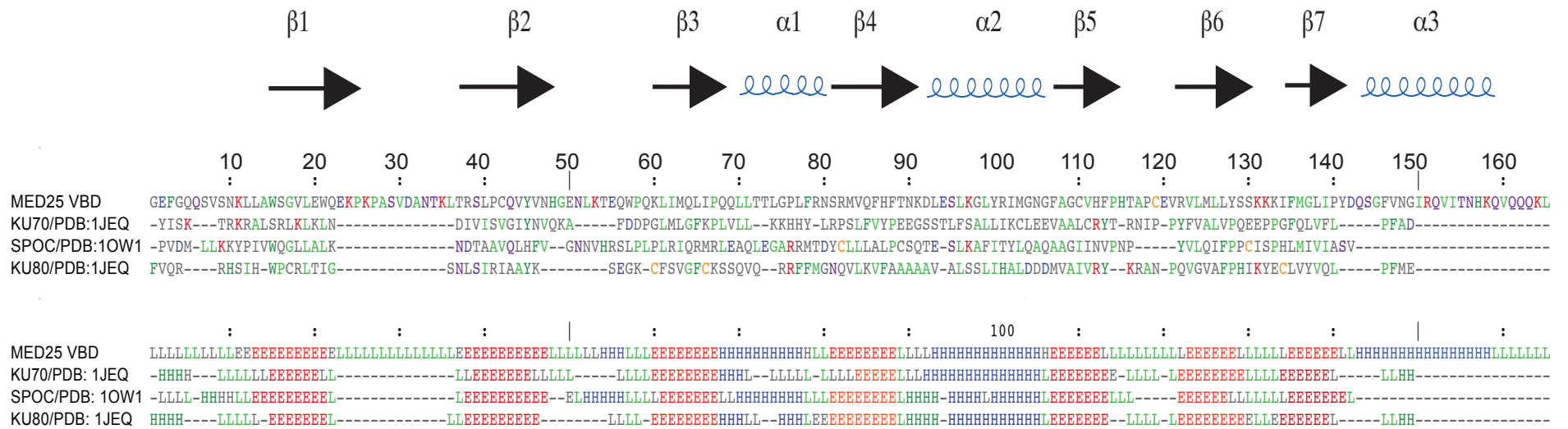
Supplementary Figure 1. Sequence alignments of the MED25 VBD and VP16 TAD. **(a)** Sequence of the human MED25 VBD aligned with the homologous C- and N-terminal domain of human PTOV1. Secondary structure elements are shown above the sequences. **(b)** Sequence of the VP16 TAD from *Herpes simplex virus 1* aligned with sequences of TADs from other viruses. Alignments were visualized with ESPript¹. Conserved residues are highlighted in red.



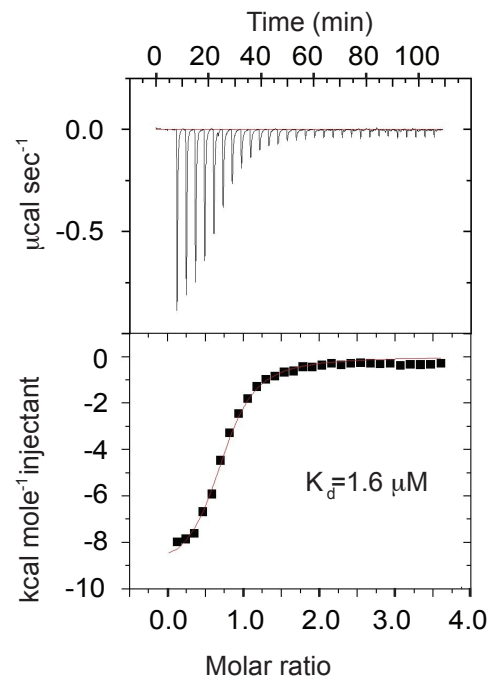
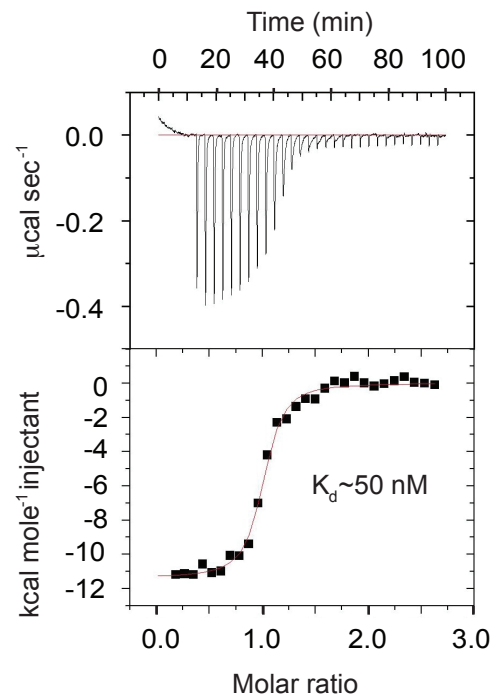
Supplementary Figure 2. ^1H - ^{15}N -HSQC spectrum of the MED25 VBD with the assigned residue numbers.



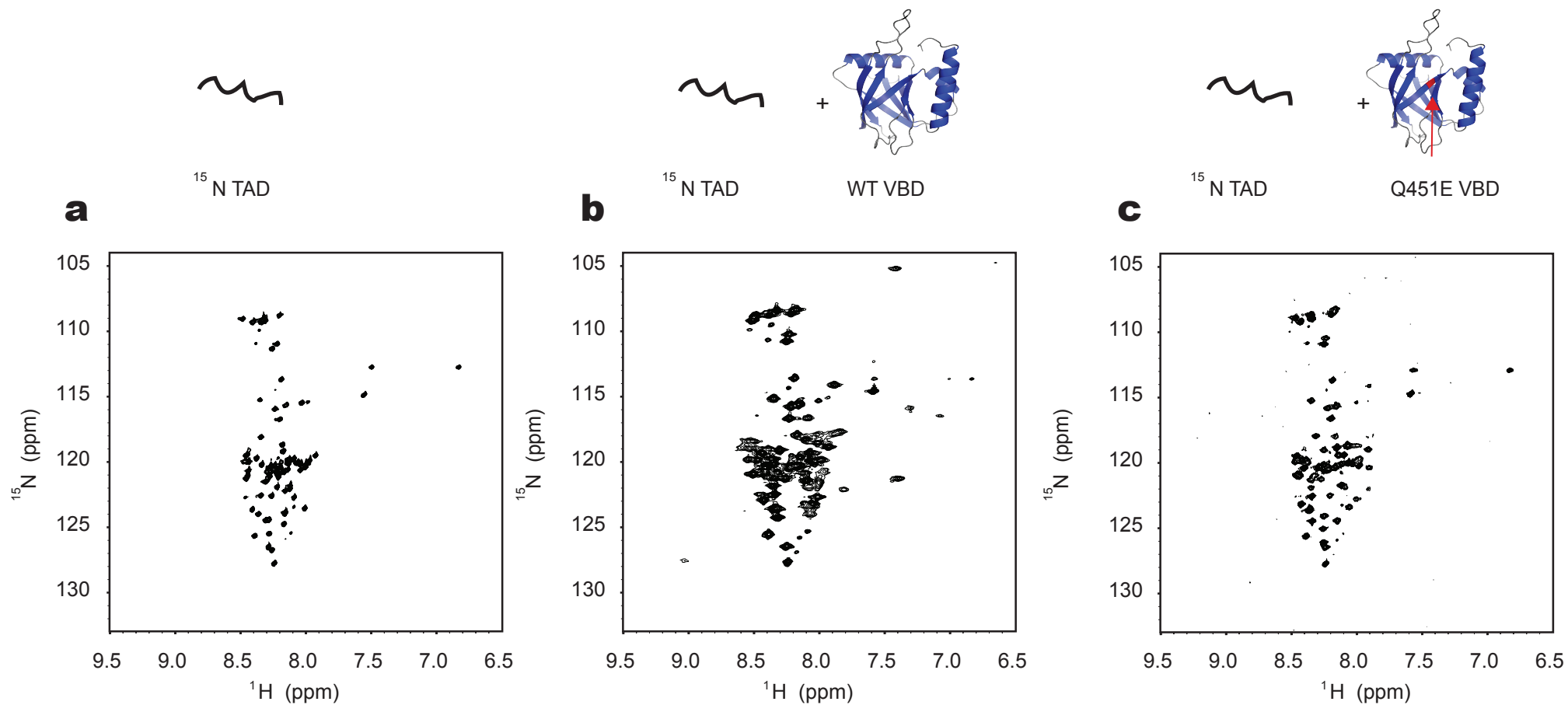
Supplementary Figure 3. ^{15}N T_2 relaxation time measurement of the MED25 VBD. **(a)** ^{15}N T_2 relaxation times of the free MED25 VBD are plotted against the residue number. Error bars represent s.d. The N- and C-terminus and the long loop between $\beta 1$ and $\beta 2$ display significantly longer T_2 times, indicating local flexibility. Due to line broadening and peak overlap, T_2 times of the residues forming loop $\beta 5/ \beta 6$ could only be determined for T503. **(b)** The 25 lowest energy structures are shown overlaid on the secondary structure elements. Loop $\beta 2/ \beta 3$ and loop $\beta 5/ \beta 6$ close the barrel from the bottom.



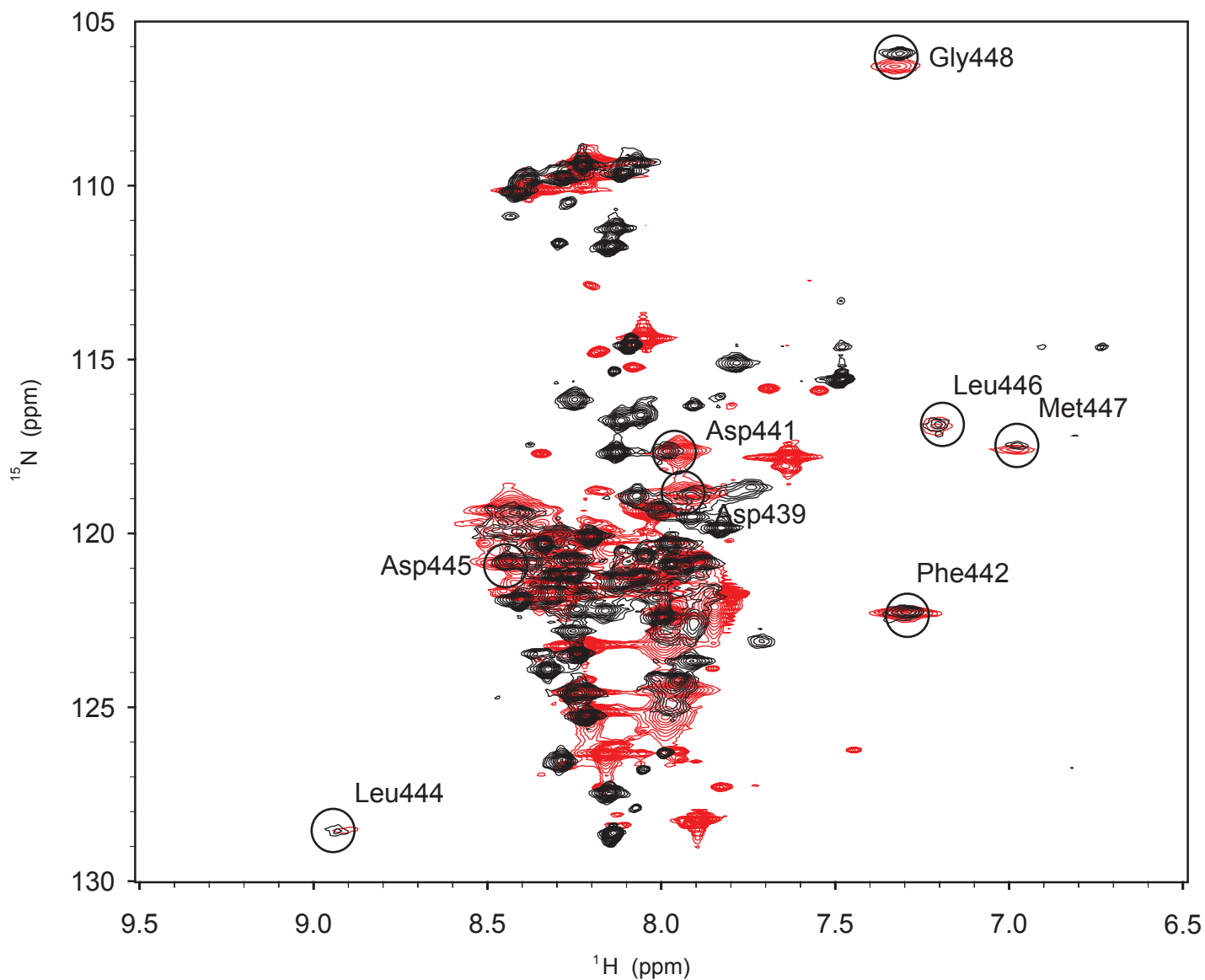
Supplementary Figure 4. Structural homology search by DALI². Alignment of amino acid sequences (upper panel) and structural elements (lower panel) with the three structural homologous proteins of MED25 VBD: KU70/PDB: 1JEQ³, SPOC/PDB: 1OW1⁴, KU80/PDB:1JEQ³. Extended regions are highlighted in red and helical portions are shown in blue (lower panel).

a**b**

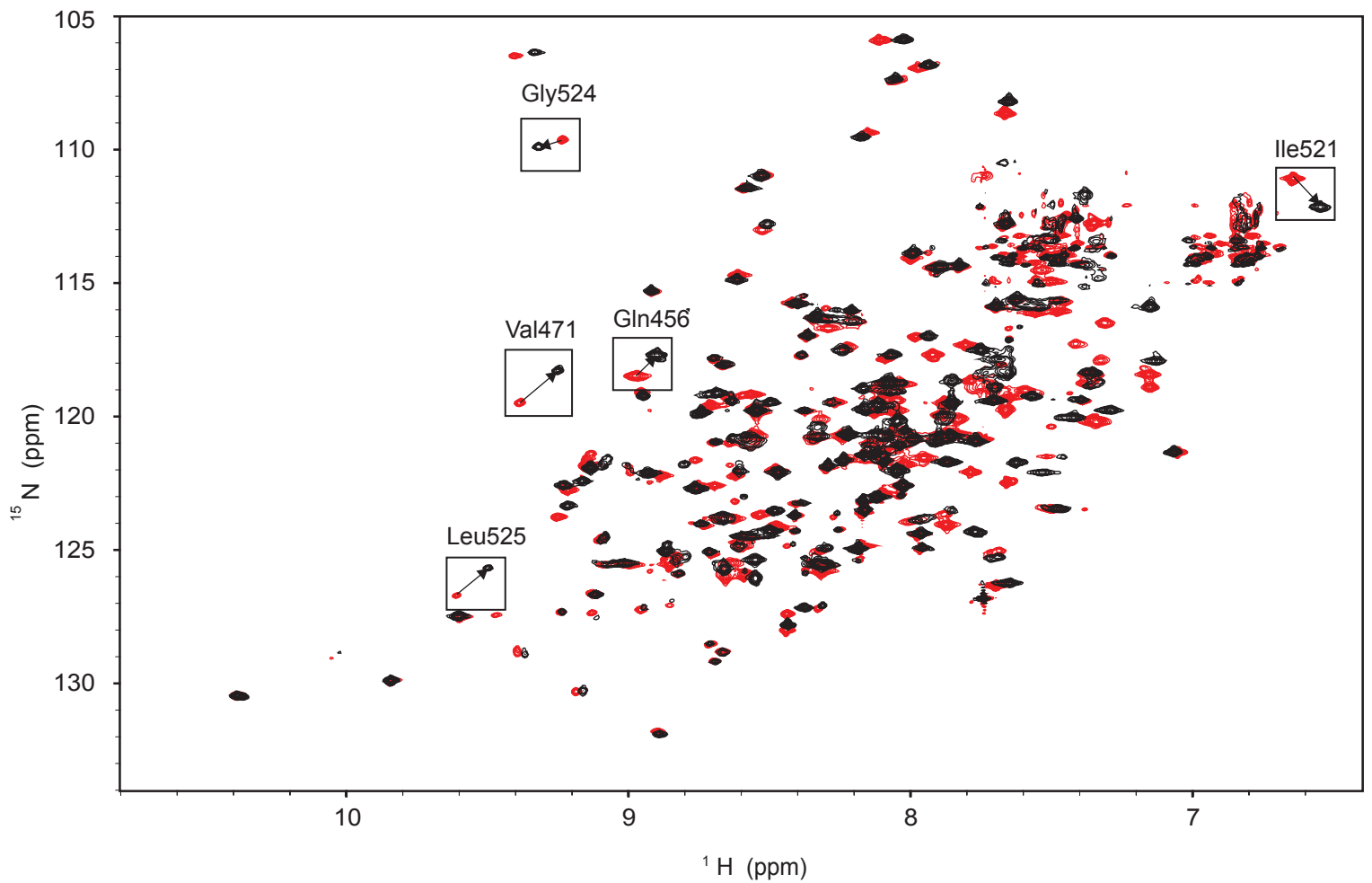
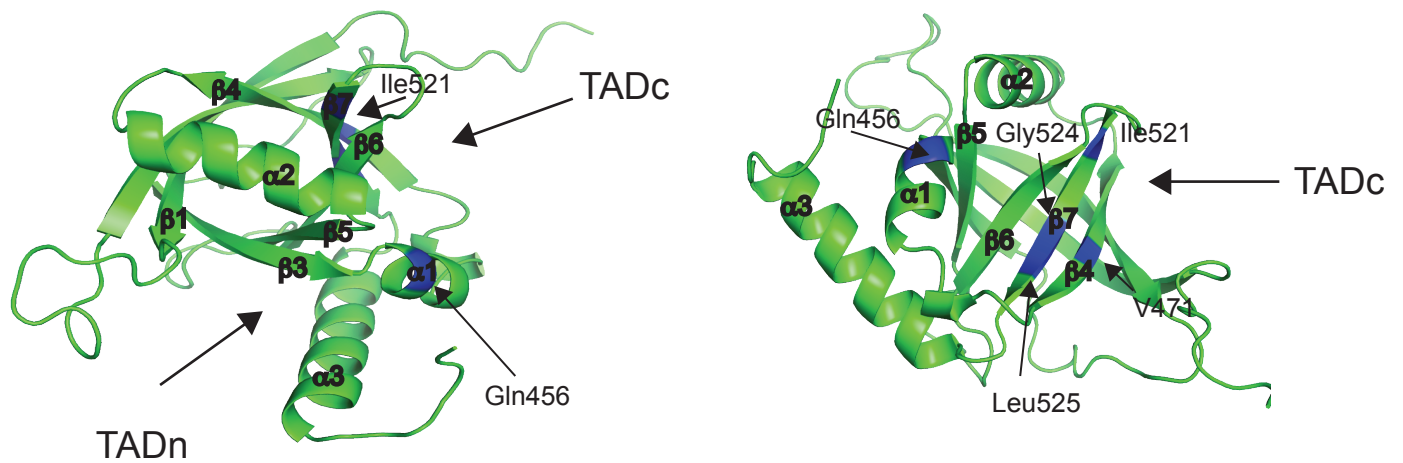
Supplementary Figure 5. Isothermal calorimetry titration. **(a)** Isothermal calorimetry titration of MED25 VBD with VP16 TADn revealed a K_d of 1.6 μM . **(b)** Isothermal calorimetry titration of MED25 VBD with VP16 full-length TAD revealed a K_d of approximately 50 nM. The C-terminal portion of the VP16 TAD contributes to the binding to MED25 VBD and likely accounts for the difference in K_d between TADn and TAD.



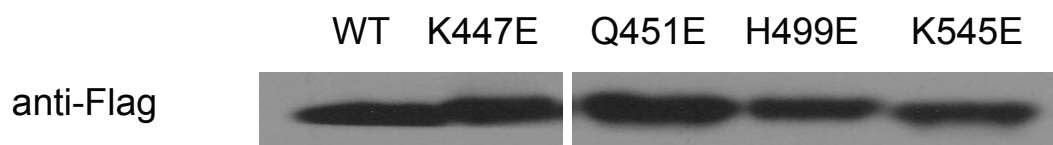
Supplementary Figure 6. The MED25 VBD Q451E mutation on $\beta 3$ adjacent to the hydrophobic pocket also disrupts binding of full-length VP16 TAD to MED25 VBD. ^1H - ^{15}N -HSQC spectra of free VP16 TAD (**a**), at 1:1 ratio of wild-type MED25 VBD (**b**) and with 1:1.5 excess of Q451E MED25 VBD (**c**) show that VP16 TAD only loosely binds, as seen by minor chemical shift changes, to mutant MED25 VBD without adopting a folded conformation. Far-shifted and broadened signals caused by the addition of wild-type MED25 VBD (**b**), are missing when the mutant MED25 VBD is added to ^{15}N -labeled VP16 TAD (**c**).



Supplementary Figure 7. ^1H - ^{15}N -HSQC spectra of the VP16 TAD (black signals) and the VP16 TADn (red signals) in the presence of 1.3 equivalents MED25 VBD. Far-shifted resonances overlap for both peptides and are indicated by circles and assignment.

a**b**

Supplementary Figure 8. Mapping the TADc binding site on MED25 VBD. **(a)** Overlay of ^1H - ^{15}N -TROSY-HSQC⁵ spectra of the MED25 VBD bound to the VP16 TADn (red) and the MED25 VBD bound to the VP16 TAD (black). **(b)** A cartoon representation shows the clustering of the residues experiencing distinct chemical shifts upon interaction with VP16 TADc on $\beta 4$ and $\beta 7$. The TADn and TADc binding sites are located on different sides of the MED25 VBD barrel.



Supplementary Figure 9. Wild-type and mutant MED25 VBD displayed comparable level of expression in transfected HEK293T cells when immunoblotted with anti-Flag antibody.

Supplementary Table 1. Ramachandran Plot Summary of the MED25 VBD structure from PROCHECK⁶.

Ramachandran Plot Summary from PROCHECK	
Most favoured regions	89.1%
Additionally allowed regions	10.4%
Generously allowed regions	0.5%
Disallowed regions	0.0%

Supplementary References

1. Gouet, P., Courcelle, E., Stuart, D.I. & Metz, F. ESPript: analysis of multiple sequence alignments in PostScript. *Bioinformatics* **15**, 305-308 (1999).
2. Holm, L. & Sander, C. Protein structure comparison by alignment of distance matrices. *J Mol Biol* **233**, 123-138 (1993).
3. Walker, J.R., Corpina, R.A. & Goldberg, J. Structure of the Ku heterodimer bound to DNA and its implications for double-strand break repair. *Nature* **412**, 607-614 (2001).
4. Ariyoshi, M. & Schwabe, J.W. A conserved structural motif reveals the essential transcriptional repression function of Spen proteins and their role in developmental signaling. *Genes Dev* **17**, 1909-1920 (2003).
5. Pervushin, K., Riek, R., Wider, G. & Wüthrich, K. Attenuated T2 relaxation by mutual cancellation of dipole-dipole coupling and chemical shift anisotropy indicates an avenue to NMR structures of very large biological macromolecules in solution. *Proc Natl Acad Sci U S A* **94**, 12366-12371 (1997).
6. Laskowski, R.A., Rullmann, J.A., MacArthur, M.W., Kaptein, R. & Thornton, J.M. AQUA and PROCHECK-NMR: programs for checking the quality of protein structures solved by NMR. *J Biomol NMR* **8**, 477-486 (1996).